



**HAL**  
open science

# Classical swine fever virus npro limits type I interferon induction in plasmacytoid dendritic cells by interacting with interferon regulatory factor 7

Ana R Fiebach, Laurence Guzylack-Piriou, Sylvie Python, Artur Summerfield, Nicolas Ruggli

## ► To cite this version:

Ana R Fiebach, Laurence Guzylack-Piriou, Sylvie Python, Artur Summerfield, Nicolas Ruggli. Classical swine fever virus npro limits type I interferon induction in plasmacytoid dendritic cells by interacting with interferon regulatory factor 7. *Journal of Virology*, 2011, 85 (16), pp.8002-8011. 10.1128/JVI.00330-11 . hal-01191121

**HAL Id: hal-01191121**

**<https://hal.science/hal-01191121>**

Submitted on 14 Nov 2015

**HAL** is a multi-disciplinary open access archive for the deposit and dissemination of scientific research documents, whether they are published or not. The documents may come from teaching and research institutions in France or abroad, or from public or private research centers.

L'archive ouverte pluridisciplinaire **HAL**, est destinée au dépôt et à la diffusion de documents scientifiques de niveau recherche, publiés ou non, émanant des établissements d'enseignement et de recherche français ou étrangers, des laboratoires publics ou privés.

# Classical Swine Fever Virus N<sup>pro</sup> Limits Type I Interferon Induction in Plasmacytoid Dendritic Cells by Interacting with Interferon Regulatory Factor 7<sup>∇</sup>

Ana R. Fiebach,<sup>†</sup> Laurence Guzylack-Piriou,<sup>†‡</sup> Sylvie Python,  
Artur Summerfield,\* and Nicolas Ruggli\*

*Institute of Virology and Immunoprophylaxis, Mittelhäusern, Switzerland*

Received 17 February 2011/Accepted 23 May 2011

Viruses are detected by different classes of pattern recognition receptors that lead to the activation of interferon regulatory factors (IRF) and consequently to the induction of alpha/beta interferon (IFN- $\alpha/\beta$ ). In turn, efficient viral strategies to escape the type I IFN-induced antiviral mechanisms have evolved. Previous studies established that pestivirus N<sup>pro</sup> antagonizes the early innate immune response by targeting the transcription factor IRF3 for proteasomal degradation. Here, we report that N<sup>pro</sup> of classical swine fever virus (CSFV) interacts also with IRF7, another mediator of type I IFN induction. We demonstrate that the Zn-binding domain of N<sup>pro</sup> is essential for the interaction of N<sup>pro</sup> with IRF7. For IRF3 and IRF7, the DNA-binding domain, the central region, and most of the regulatory domain are required for the interaction with N<sup>pro</sup>. Importantly, the induction of IRF7-dependent type I IFN responses in plasmacytoid dendritic cells (pDC) is reduced after wild-type CSFV infection compared with infection with virus mutants unable to interact with IRF7. This is associated with lower levels of IRF7 in pDC. Consequently, wild-type but not N<sup>pro</sup> mutant CSFV-infected pDC show reduced responses to other stimuli. Taken together, the results of this study show that CSFV N<sup>pro</sup> is capable of manipulating the function of IRF7 in pDC and provides the virus with an additional strategy to circumvent the innate defense.

Innate immune activation following viral infection is dependent on recognition by pattern recognition receptors (PRRs) and on the production of alpha/beta interferon (IFN- $\alpha/\beta$ ) (32, 38). Toll-like receptors (TLR) and the cytosolic RIG-I and MDA5 recognize viral RNA (11, 31, 58) and respond by activating a signaling network that culminates in the induction of type I IFN and establishes an antiviral state (22). The central players of this signaling cascade are interferon regulatory factor 3 (IRF3) and IRF7. They are essential to modulate the activity of the innate immune response (45, 55) but have distinct roles in the induction of IFN-stimulated genes. As a result of the signaling initiated by the cytoplasmic PRRs, IRF3 is phosphorylated by the kinases IKK $\epsilon$  and TANK-binding kinase 1, dimerizes, and translocates to the nucleus, where it eventually upregulates transcription of IFN- $\alpha/\beta$  mRNA (13, 50). TLR7, TLR8, and TLR9 trigger the induction of IFN- $\alpha$  through the adaptor molecule MyD88, which forms a complex with IRF7 in pDC (33). IRF7 is in turn phosphorylated by interleukin-1 (IL-1) receptor-associated kinase (IRAK)-1 and translocates to the nucleus (56). IRF3 is expressed mainly constitutively and appears to be an important element in the early phase of the IFN- $\alpha/\beta$  induction. In contrast, IRF7 is a protein with a short half-life that is usually expressed at low

levels, but it is highly inducible by type I IFN (20) and hence is expressed in larger amounts in the later phase of the type I IFN induction (19, 36, 45). However, in mice, constitutive expression of IRF7 in plasmacytoid dendritic cells (pDC) enables them to render fast and efficient IFN- $\alpha/\beta$  responses (24). Furthermore, pDC are the only cell type described to produce type I IFN in IRF3 knockout mice (24).

During evolution, viruses have acquired numerous mechanisms to evade or subvert key elements of the host viral response (15, 19, 21, 57). For pestiviruses, it is known that they counteract the IFN- $\alpha/\beta$  induction by mediating the proteasomal degradation of IRF3 in their primary target cells, such as myeloid DC and endothelial and epithelial cells, allowing the virus to establish a productive infection (6, 9, 23, 48). The viral protein responsible for this function is N<sup>pro</sup>, encoded at the N terminus of the single open reading frame of the positive-sense RNA genome. N<sup>pro</sup> harbors an autoprotease domain in the N-terminal half of the protein, resulting in cotranslational release of N<sup>pro</sup> from the nascent polyprotein. In the C-terminal half of N<sup>pro</sup>, a metal-binding TRASH motif consisting of C<sub>112</sub>-X<sub>21</sub>-C<sub>134</sub>-X<sub>3</sub>-C<sub>138</sub> mediates the coordination of one zinc (Zn) atom per molecule (53). This domain is essential for N<sup>pro</sup> to interact with IRF3 and to mediate the degradation of IRF3 by the proteasome.

In the present study, we identified IRF7 as a novel interaction partner of N<sup>pro</sup>. We show that N<sup>pro</sup> modulates the IRF7 turnover, limiting the IFN- $\alpha$  induction in pDC, which is of functional relevance for pathogenesis.

\* Corresponding author. Mailing address: Institute of Virology and Immunoprophylaxis (IVI), Sensemattstrasse 293, CH-3147 Mittelhäusern, Switzerland. Phone: 41 31 848 9211. Fax: 41 31 848 9222. E-mail for Nicolas Ruggli: nicolas.ruggli@ivi.admin.ch. E-mail for Artur Summerfield: artur.summerfield@ivi.admin.ch.

<sup>†</sup> These authors contributed equally.

<sup>‡</sup> Present address: Institut National de la Recherche Agronomique, 180 Chemin de Tournefeuille, F-31027 Toulouse, France.

<sup>∇</sup> Published ahead of print on 15 June 2011.

## MATERIALS AND METHODS

**Cells.** The porcine kidney cell lines SK-6 (30) and PK-15 (ATCC) were propagated in Earle's minimal essential medium (EMEM) with 7% horse serum and

in Dulbecco's minimal essential medium (DMEM) supplemented with 5% horse serum, nonessential amino acids, and 1 mM Na pyruvate. HEK293T cells (ATCC) were cultured in EMEM supplemented with 10% fetal bovine serum (Biochrom AG). Peripheral blood mononuclear cells (PBMC) were obtained from blood of specific-pathogen-free pigs using Ficoll-Paque density centrifugation (1.077 g/liter; Amersham Pharmacia Biotech). pDC were enriched as described previously (18) by cell sorting of CD172a<sup>+</sup> PBMC using the magnetic cell sorting system (MACS) with LD columns (Miltenyi Biotec GmbH). This permits a 10-fold enrichment of functional pDC to 2 to 5% (52). To obtain a purified pDC preparation, PBMC were centrifuged over a 1.065-density iodixanol gradient (Optiprep; Nycomed Pharma) (47). Subsequently, the cells were depleted of T cells using anti-CD3, followed by CD4 enrichment on LS columns (MACS). This protocol yielded 60 to 80% pure pDC, identified as CD4<sup>high</sup> CD172a<sup>low</sup> (17).

**Viruses.** The classical swine fever virus (CSFV) strains vA187-1 and vA187-ΔN<sup>PRO</sup> (44) were derived from the respective full-length cDNA clones. The vA187-1-derived viruses vA187-C<sub>112</sub>R and vA187-D<sub>136</sub>N (referred to as the C<sub>112</sub>R and D<sub>136</sub>N mutants, respectively) with single-amino-acid mutations in N<sup>PRO</sup> were described previously (43). All virus titers were determined on SK-6 and PK-15 cells by standard endpoint dilution and were expressed as 50% tissue culture infectious doses (TCID<sub>50</sub>) per ml. The avian influenza virus H5N1 NIBRG14, used for stimulation of pDC, was obtained from Jim Robertson (National Institute for Biological Standards and Control, Hertfordshire, United Kingdom).

**Plasmid constructs.** The plasmids pCI-Ub-Core, pFLAG-IRF3, and pFLAG-IRF7 were described elsewhere (6, 42). For the mammalian two-hybrid assays (Promega), plasmid pFN10A(ACT)-IRF3 expressing the porcine IRF3 fused to the VP16 transactivator domain and pFN11A(BIND)-derived plasmids expressing GAL4-N<sup>PRO</sup> and the mutants GAL4-N<sup>PRO</sup>(C<sub>69</sub>A), N<sup>PRO</sup>(C<sub>112</sub>R), N<sup>PRO</sup>(C<sub>134</sub>A), N<sup>PRO</sup>(D<sub>136</sub>N), N<sup>PRO</sup>(C<sub>138</sub>A), and N<sup>PRO</sup>(C<sub>161</sub>A) were used; these are described elsewhere (43, 53). Mutants with deletions in the IRF3 and IRF7 genes were obtained by PCR-based site-directed mutagenesis using standard techniques. Briefly, the mutants were constructed using the plasmids pIRF3 and pFLAG-IRF7 (6). Mutagenesis was performed by PCR with appropriate oligonucleotides (Microsynth) and AccuPrime Pfx DNA polymerase (Invitrogen). The integrity of the mutagenized DNA fragments was verified by nucleotide sequencing using the Thermo Sequenase DYEnamic direct cycle sequencing kit (GE Healthcare) and the Global IR2 System with e-Seq software (Li-Cor Biosciences).

**Antibodies.** The rabbit polyclonal antisera against recombinant affinity-purified CSFV N<sup>PRO</sup> (42), CSFV C, and porcine IRF3 were described previously (6). The viral nonstructural protein NS3 was detected using the monoclonal antibody (MAb) C16 (16), kindly provided by Irene Greiser-Wilke, Hannover Veterinary School, Hannover, Germany. The anti-FLAG M2 MAb and the anti-α-tubulin MAb were purchased from Sigma. The antiserum against the porcine IRF7 was produced in rabbits with a recombinant protein encompassing amino acids 122 to 487 of the porcine IRF7 expressed in *Escherichia coli* M15 with the pQE31 vector (Qiagen) and purified by nickel chelate affinity chromatography as described previously for N<sup>PRO</sup> (42). For pDC phenotyping and isolation, MAbs against the following cell surface molecules were used: CD172a (MAb 74-22-15A), CD4 (MAb 74-12-4 and PT90A), and CD3 (MAb PPT3). Hybridomas for MAbs 74-22-15A and 74-12-4 were kindly donated by Armin Saalmüller (Institute of Immunology, Department of Pathobiology, University of Veterinary Medicine, Vienna, Austria), and the hybridoma for MAb PPT3 was a gift from Karin Haverson (University of Bristol, United Kingdom). MAb PT90A was purchased from VMRD (Pullman, WA).

**Immunoprecipitation.** Coimmunoprecipitation was performed essentially as described by Rottenberg et al (41). Briefly, cells were lysed for 20 min on ice with a buffer containing 20 mM Tris (pH 7.4), 75 mM NaCl, 0.1% Triton X-100, and 2.5 mM MgCl<sub>2</sub>, supplemented with 5 μl/ml protease inhibitor cocktail (BD) and 10 μl/ml phosphatase inhibitor cocktail II (Sigma). After clarification by centrifugation at 15'000 × g for 10 min at 4°C, the lysates were incubated overnight at 4°C with 50 μl anti-FLAG M2 agarose (Sigma) in Tris-buffered saline (TBS) (20 mM Tris-HCl, 75 mM NaCl, pH 7.6). After incubation, the agarose was washed three times with TBS and the protein complexes were eluted from the beads with 20 μl of 2× sample buffer (125 mM Tris-HCl, pH 6.8, 20% glycerol, 1% bromophenol blue, 4% sodium dodecyl sulfate [SDS]). The eluted proteins were analyzed by sodium dodecyl sulfate-polyacrylamide gel electrophoresis (SDS-PAGE) and Western blotting.

**SDS-PAGE and Western blotting.** Cells were lysed in a hypotonic buffer containing 20 mM morpholinepropanesulfonic acid, 10 mM NaCl, 1.5 mM MgCl<sub>2</sub>, 1% Triton X-100 (pH 6.5), and 1 μl/10<sup>6</sup> cells protease inhibitor cocktail (Sigma). Proteins were separated by SDS-PAGE under reducing conditions and

analyzed by Western blotting as previously described (43). The signal was acquired using the Odyssey infrared imaging system (Li-Cor Biosciences).

**FCM analysis.** The detection of the viral NS3 protein and the porcine IRF3 and IRF7 by flow cytometry (FCM) was performed as described previously (6). For staining of cell surface molecules, unfixed cells were incubated for 20 min on ice with the respective primary and secondary antibodies diluted in Cellwash (Becton Dickinson). For the detection of the intracellular antigens NS3, IRF3, and IRF7, the cells were fixed and permeabilized with FIX&PERM solution (An der Grub Bio Research GmbH) and stained with rabbit anti-NS3, anti-IRF3, and anti-IRF7 polyclonal antibody. For detection by FCM, isotype-specific fluorescein isothiocyanate (FITC), R-phycoerythrin (RPE) (Southern Biotechnology Associates), and RPE-Cy5 (Dako) conjugates were used as described previously (17).

**Mammalian two-hybrid assay.** Protein interactions were analyzed with the CheckMate/Flexi Vector mammalian two-hybrid system (Promega) as described before (43). Briefly, HEK293T cells were seeded at a density of 10<sup>5</sup> cells/well in a 24-well plate. One day later, the cells were transfected with a mixture of the pFN10A(ACT)-derived and pFN11A(BIND)-derived plasmids at a concentration of 100 ng/well each and the pGL4.31(luc2P/GAL4UAS/Hygro) reporter plasmid (Promega) at 50 ng/well. The plasmids pACT-Myo and pBind-Id (Promega) were used as controls. The transfections were performed with FuGENE 6 transfection reagent (Roche) according to the manufacturer's protocol. After 48 h of incubation at 37°C, the cells were lysed with passive lysis buffer (Promega). Firefly and *Renilla* luciferases were quantified using the dual luciferase reporter assay system (Promega). The relative luminescence measured with firefly luciferase induced from the reporter plasmid was normalized with the corresponding relative luminescence obtained with *Renilla* luciferase constitutively expressed from the pFN11A(BIND)-derived plasmid. The fold firefly luciferase induction was calculated relative to the normalized firefly luciferase activity obtained with the empty vectors set to 1. The expression of the proteins fused to VP16 and GAL4 was analyzed by SDS-PAGE and Western blotting as described above.

**Type I IFN detection.** The bioactivity of porcine IFN-α/β in SK-6 cells was assayed as described previously (42, 44) using the Mx/CAT reporter gene assay developed for the quantification of bovine IFN-α/β (14) and kindly provided by Martin D. Fray (Institute of Animal Health, Compton, Newbury, Berkshire, United Kingdom). To this end, the culture supernatants were added to MDBK-t2 cells at appropriate dilutions allowing measurement in the linear range of the assay. Recombinant porcine IFN-α produced in HEK293-EBNA cells (4) was used as standard. Chloramphenicol acetyltransferase (CAT) was quantified using a CAT enzyme-linked immunosorbent assay (ELISA) (Roche). For the detection of IFN-α in purified pDC, the cells were stimulated with CpG 2216 at 10 μg/ml or with avian influenza virus (AIV) strain H5N1 NIBRG-23 for 24 h. Secreted IFN-α was detected by ELISA using anti-pig IFN-α MAbs K9 and F17 (kindly provided by Bernard Charley, INRA, Jouy-en-Josas, France) as described previously (18).

**RNA extraction and quantitative TaqMan RT-PCR for porcine IRF3, IRF7, and IFN-β.** To determine mRNA levels in pDC, total RNA was prepared using the RNeasy minikit (Qiagen, Hombrechtikon, Switzerland), followed by treatment with RNase-free DNase I (Ambion, Huntingdon, United Kingdom). Reverse transcription-PCR (RT-PCR) was performed using the ABI PRISM 7700 sequence detector system (Applied Biosystems, Foster City, CA). The oligonucleotides for the quantification of IRF7 and 18S mRNAs were designed based on the coding sequence of the respective genes using Primer Express version 1.5 software (Applied Biosystems). The sense IRF7 primer 5'-CTGCCGATGGCTG GATGAA-3' and the antisense IRF7 primer 5'-TAAAGATGCGCGAGTCGG A-3' were used in combination with the IRF7 probe 5'-CCGCGTGCCCTGGA AGCATT-3'. The sense 18S primer 5'-CGCCGCTAGAGGTGAAATTC-3' and the antisense 18S primer 5'-GGCAAATGCTTTCGCTCTG-3' were used together with the 18S probe 5'-TGGACCCGGCGAAGACGGA-3'. The relative expression of each mRNA was determined with the ΔC<sub>T</sub> method by calculating the amount of target mRNA in relation to 18S mRNA. The data are presented as the ratio of target mRNA to 18S mRNA.

## RESULTS

**N<sup>PRO</sup> interacts with IRF7.** Pestivirus N<sup>PRO</sup> inhibits dsRNA-mediated IFN-α/β induction by mediating the proteasomal degradation of IRF3 (6, 9, 23). Although N<sup>PRO</sup> does not accelerate the degradation of IRF7 expressed exogenously (6), we investigated whether N<sup>PRO</sup> interferes with the functions of IRF7

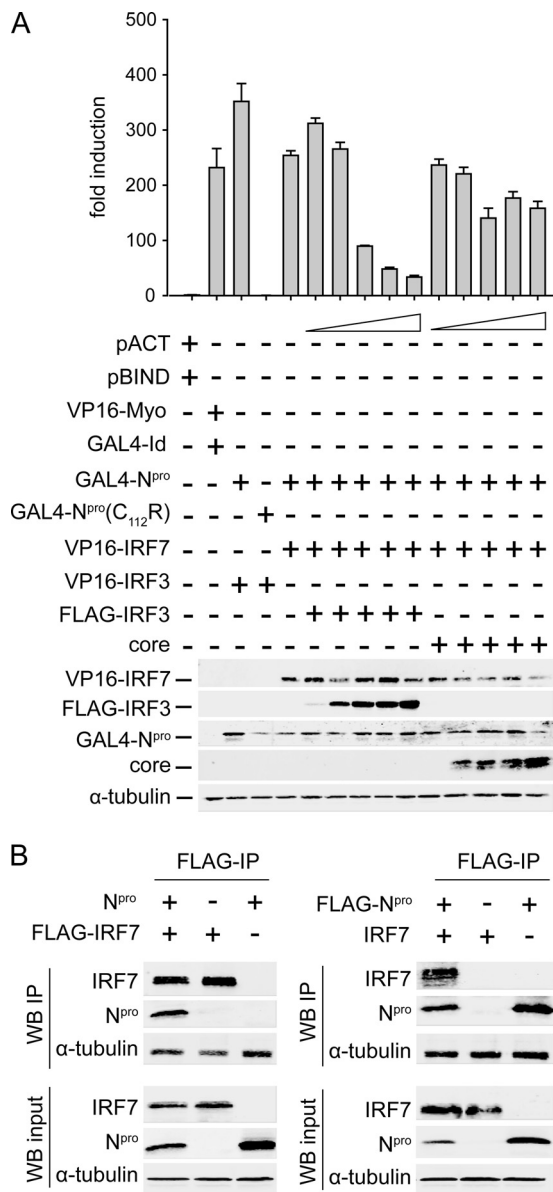


**FIG. 1.** N<sup>PRO</sup> interacts with IRF7. The interaction of N<sup>PRO</sup> with IRF7 was analyzed using a mammalian two-hybrid assay (A) and by immunoprecipitation (B). (A) For the mammalian two-hybrid assay, HEK293T cells were cotransfected with pFN10A(ACT)-derived plasmids expressing IRF7 or IRF3 fused to the VP16 transactivator (VP16-IRF7 and VP16-IRF3, respectively) and with pFN11A(BIND)-derived plasmids expressing the viral N<sup>PRO</sup> or the N<sup>PRO</sup>(C<sub>112</sub>R) mutant fused to the GAL4 DNA-binding domain [GAL4-N<sup>PRO</sup> and GAL4-N<sup>PRO</sup>(C<sub>112</sub>R), respectively]. These constructs were transfected alone or in combination with increasing amounts of 1 ng, 25 ng, 100 ng, 250 ng, and 500 ng (indicated with open triangles) of plasmids for CMV promoter-driven expression of FLAG-IRF3 or of the C protein (core) of CSFV. The presence and the absence of the plasmids are indicated with + and -, respectively. The empty vectors pACT and pBIND served as negative controls, whereas the VP16-Myo and GAL4-Id control proteins expressed from pFN10A(ACT) and pFN11A(BIND), respectively, were used as positive controls. After 48 h of incubation, the cells were lysed and the firefly luciferase activity was measured and normalized with *Renilla* luciferase activity constitutively expressed by the pFN11A(BIND)-plasmid. The results are shown as fold induction compared to the negative control and represent the mean of triplicates from a representative experiment, with error bars showing the standard deviation. In parallel, the VP16-IRF7, FLAG-IRF3, GAL4-N<sup>PRO</sup>,

by other means. We used a mammalian two-hybrid assay to analyze whether N<sup>PRO</sup> can interact with IRF7, using IRF3 as a control. As expected from previous experiments, coexpression of N<sup>PRO</sup> fused to the GAL4 DNA-binding domain and of IRF3 fused to the VP16 activation domain resulted in strong induction of GAL4 promoter-driven luciferase expression compared with that with the empty vectors (Fig. 1A). The C<sub>112</sub>R mutation in N<sup>PRO</sup> completely abolished this interaction, as shown before (43). In the same assay, coexpression of N<sup>PRO</sup> with porcine IRF7 also produced a strong induction of luciferase expression, indicating an interaction of N<sup>PRO</sup> with IRF7. Importantly, coexpression of increasing amounts of FLAG-IRF3 diminished the interaction of N<sup>PRO</sup> with IRF7 gradually, confirming the specificity of the interaction between N<sup>PRO</sup> and IRF7. While an excess of IRF3 displaced IRF7, the cotitration of the C protein of CSFV as a control had no influence on the interaction of N<sup>PRO</sup> with IRF7 (Fig. 1A). To further confirm these findings, HEK293T cells were cotransfected with plasmids expressing FLAG-IRF7 and untagged N<sup>PRO</sup> or with each plasmid individually, and proteins were coimmunoprecipitated with anti-FLAG agarose. N<sup>PRO</sup> was immunoprecipitated with anti-FLAG from cell lysates containing both FLAG-IRF7 and untagged N<sup>PRO</sup> but not from cells expressing N<sup>PRO</sup> or FLAG-IRF7 alone (Fig. 1B). Conversely, IRF7 was immunoprecipitated with anti-FLAG from cell lysates containing both FLAG-N<sup>PRO</sup> and untagged IRF7 but not when these proteins were expressed alone (Fig. 1B). These experiments show that N<sup>PRO</sup> interacts with IRF7.

**The Zn-binding domain of N<sup>PRO</sup> is required for the interaction with IRF7.** A recent report described a novel Zn-binding TRASH motif in N<sup>PRO</sup>, involving the residues C<sub>112</sub>, C<sub>134</sub>, D<sub>136</sub>, and C<sub>138</sub>. Zn binding by N<sup>PRO</sup> is a prerequisite for the interaction of N<sup>PRO</sup> with IRF3, leading to the proteasomal degradation of IRF3 and to the inhibition of type I IFN induction (53). Considering the structural similarity of IRF3 and IRF7, we asked whether N<sup>PRO</sup> also relies on the same Zn-binding domain to interact with IRF7. To this end we analyzed the interaction of TRASH domain mutants of N<sup>PRO</sup> with porcine IRF3 and IRF7, using the mammalian two-hybrid assay. Coexpression of GAL4-N<sup>PRO</sup> and VP16-IRF3 or of GAL4-N<sup>PRO</sup> and VP16-IRF7 caused a strong induction of the GAL4 promoter-driven luciferase compared to the negative control, as expected (Fig. 2). The mutations C<sub>112</sub>R, C<sub>112</sub>A, C<sub>134</sub>A, D<sub>136</sub>N, and C<sub>138</sub>A, which disrupt the TRASH domain, resulting in proteins incapable of coordinating Zn, completely abolished the interaction of N<sup>PRO</sup>

core, and α-tubulin proteins from the cells used for luciferase quantification were analyzed by Western blotting and detection with rabbit antisera against the porcine IRF7, the viral N<sup>PRO</sup>, and core and with anti-FLAG and anti-α-tubulin MAbs. (B) For immunoprecipitation, HEK293T cells were transfected with plasmids expressing FLAG-tagged IRF7 and untagged N<sup>PRO</sup> together or individually (left panels) or FLAG-tagged N<sup>PRO</sup> and untagged IRF7 together or individually (right panels). At 24 h after transfection, the cells were lysed and the FLAG-tagged proteins were immunoprecipitated (FLAG-IP) with anti-FLAG M2 agarose. The precipitated proteins (IP) and the lysates subjected to the immunoprecipitation (input) were analyzed by Western blotting (WB) and detection using the anti-N<sup>PRO</sup> rabbit antiserum, the anti-FLAG MAb, and the anti-α-tubulin MAb as indicated.

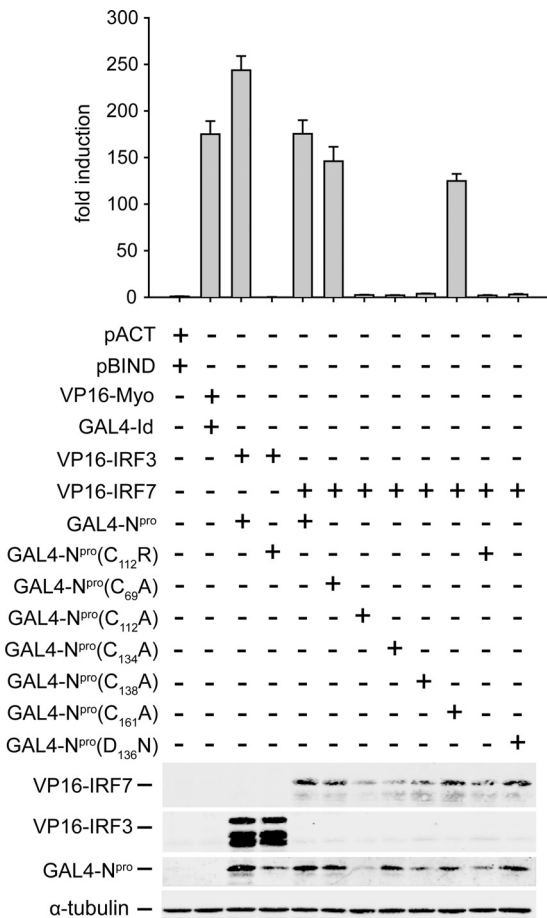


FIG. 2. The zinc-binding TRASH domain of N<sup>PRO</sup> is essential for the interaction of N<sup>PRO</sup> with IRF7. HEK293T cells were cotransfected with pFN10A(ACT)-derived plasmids expressing VP16-IRF3 or VP16-IRF7 and with pFN11A(BIND)-derived plasmids for the expression of GAL4-N<sup>PRO</sup> or the indicated mutants thereof. The empty vectors pACT and pBIND were used as negative controls, and the respective plasmids expressing VP16-Myo and GAL4-Id served as positive controls. The presence and the absence of the plasmids are indicated with + and -, respectively. The fold induction of firefly luciferase activity normalized to *Renilla* luciferase activity was calculated relative to the negative control. The error bars represent the standard deviation. The expression of VP16-IRF7, VP16-IRF3, and GAL4-N<sup>PRO</sup> was analyzed in parallel from the cells used for luciferase quantification by Western blotting and detection with rabbit antisera against the porcine IRF3 and IRF7 and the viral N<sup>PRO</sup>, respectively. The α-tubulin content was determined as loading control using the anti-α-tubulin MAb.

with IRF7. Consistent with the results obtained earlier with IRF3 (53), mutation of C<sub>161</sub> to alanine did not disrupt the interaction with IRF7. In addition, the C<sub>69</sub>A mutation within the protease domain, which had no effect on the N<sup>PRO</sup>-mediated IRF3 degradation (43), also did not abrogate the interaction of N<sup>PRO</sup> with IRF7. The expression of the VP16-IRF3 and VP16-IRF7 chimeric proteins and of all the N<sup>PRO</sup> mutants was verified by Western blotting (Fig. 2). These data indicate that the Zn-binding domain but not the protease domain is required for the interaction of N<sup>PRO</sup> with IRF7, similar to the case for IRF3.

**For IRF3 and IRF7, the DNA-binding domain, the central region, and most of the regulatory domain are required for the interaction with N<sup>PRO</sup>.** There are several examples of viruses

that inhibit type I IFN induction by antagonizing the function of more than one IRF simultaneously (5, 7, 10, 27, 37). The IRF family members share conserved features in their structural architecture and have inter- and intraspecies sequence similarities (1, 5, 26, 49). In line with this, we asked whether N<sup>PRO</sup> could recognize a common motif of the porcine IRF3 and IRF7. For this purpose we used the domain prediction programs SMART (46) and InterProScan (39) to identify and map conserved motifs in porcine IRF3 and IRF7 that may be involved in the interaction with N<sup>PRO</sup>. We found that IRF3 and IRF7 contain a highly conserved N-terminal DNA-binding domain and a variable C-terminal regulatory domain (Fig. 3A). In order to investigate which of these domains are crucial for the interaction with N<sup>PRO</sup>, we constructed deletion mutant IRF3 and IRF7 lacking the DNA-binding domain or the regulatory domain, with or without the central region (Fig. 3B). The expression of the chimeric proteins VP16-IRF3 and VP16-IRF7 and of the different deletion mutants was confirmed by Western blot analysis (Fig. 3C and D). The rabbit antisera detected multiple bands. For each construct, the presence of the VP16-IRF fusion protein with the expected molecular weight (asterisks in Fig. 3C and D) was confirmed with the anti-VP16 MAb (not shown). Lower levels of the truncated proteins IRF3(195-419), IRF7(1-132), and IRF7(133-487) than of the other proteins were detected. Transfection of larger amounts of these three plasmids did not result in the expression of more protein (data not shown), suggesting that the truncated proteins were unstable. As expected, transfection of HEK293T cells with the GAL4-N<sup>PRO</sup> and VP16-IRF3 chimeric proteins resulted in strong induction of the luciferase gene, which was completely abolished by the C<sub>112</sub>R mutant (Fig. 3E). Interestingly, the carboxy-terminal IRF3(1-114) deletion mutant and the amino-terminal IRF3(115-419) and IRF3(195-419) deletion mutants did not interact with N<sup>PRO</sup>, suggesting that the DNA-binding domain and the regulatory domain alone are not sufficient for interaction with N<sup>PRO</sup>. The mutant IRF3(1-194), encompassing the DNA-binding domain and the central region and lacking the regulatory domain, showed a weak interaction that was slightly increased when half of the regulatory domain was present in the IRF3(1-272) construct. Similar results were obtained for the interaction of N<sup>PRO</sup> with the different IRF7 deletion mutants. The IRF7(1-268), mutant in which the DNA-binding domain and the central region were maintained, resulted in weak interaction with N<sup>PRO</sup> (Fig. 3F). When part of the regulatory domain in the IRF7(1-336) construct was included, binding to N<sup>PRO</sup> was nearly completely restored. The interactions of N<sup>PRO</sup> with the truncated IRF3 and IRF7 were specific, since the C<sub>112</sub>R mutant of N<sup>PRO</sup> completely abrogated the interaction. These data indicate that nearly the complete structure of IRF3 and IRF7 rather than the DNA-binding and the regulatory domain alones is required for the interaction with N<sup>PRO</sup>.

**N<sup>PRO</sup> can inhibit IRF7-driven IFN-α/β responses in SK-6 cells.** Having demonstrated that N<sup>PRO</sup> interacts with IRF7, we asked whether this interaction enhances the degradation of IRF7. Previous studies showed that N<sup>PRO</sup> does not downregulate IRF7 expression (2, 6), in contrast to IRF3 (6, 9, 23, 48), in permanent cell lines. To have an applicable cell system to study the proteasomal degradation, we transfected SK-6 cells with plasmids expressing FLAG-IRF7 under the control of the



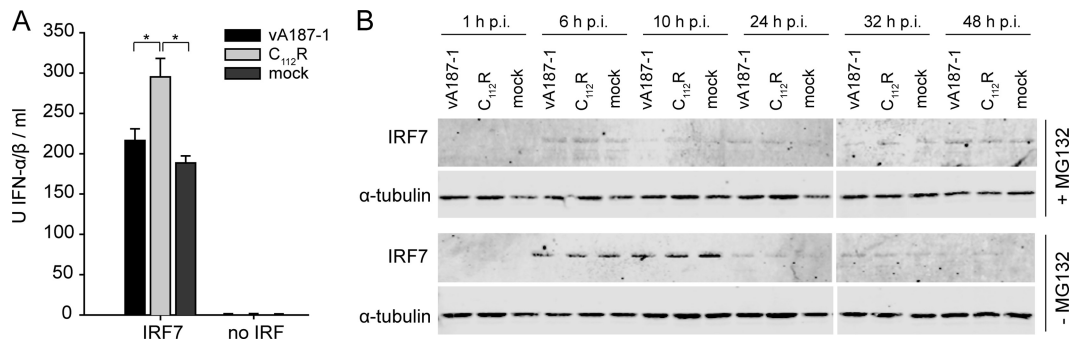


FIG. 4. N<sup>PRO</sup> does not induce proteasomal degradation of IRF7 in SK-6 cells. (A) SK-6 cells were seeded at a density of 10<sup>5</sup> cells/well and transfected with the plasmid pFLAG-IRF7 at a concentration of 100 ng/well or mock transfected (no IRF). Twenty-four hours later, the cells were mock treated or infected with CSFV vA187-1 or the C<sub>112</sub>R mutant of vA187-1 at a multiplicity of infection (MOI) of 2 TCID<sub>50</sub>/cell. After 48 h of incubation, the supernatants were collected and IFN-α/β bioactivity was measured with the MxCAT assay. Statistically significant differences (*P* < 0.05, calculated with Student's *t* test) are shown with an asterisk. (B) SK-6 cells were transfected with the plasmid pFLAG-IRF7 for CMV promoter-driven expression of FLAG-tagged porcine IRF7 in the presence (+MG132) or absence (-MG132) of 0.2 μM proteasomal inhibitor MG132. At 24 h after transfection, the cells were mock treated or infected with vA187-1 or the C<sub>112</sub>R mutant at an MOI of 2 TCID<sub>50</sub>/cell. The cells were lysed at 1, 6, 10, 24, 32, and 48 h p.i., and the extracts were analyzed for IRF7 expression using mouse anti-FLAG MAb and for α-tubulin using anti-α-tubulin MAb.

cytomegalovirus (CMV) promoter. Subsequently, the cells were mock treated or infected with vA187-1 or the C<sub>112</sub>R mutant, and IFN-α/β production was measured. Stimulation of the cells by transfection with the IRF7-expressing plasmid resulted in the production of high levels of type I IFN. Importantly, infection with the C<sub>112</sub>R mutant virus significantly enhanced IFN-α expression in IRF7-transfected cells compared with the vA187-1 virus-infected cells and mock-treated cells, indicating an inhibitory effect of N<sup>PRO</sup> on IRF7-mediated type I IFN responses to viral stimuli.

In order to analyze the effect of N<sup>PRO</sup> on IRF7 turnover, we tested how the proteasome inhibitor MG132 influences the content of IRF7 in the presence of N<sup>PRO</sup>. SK-6 cells were transfected with a plasmid expressing FLAG-tagged IRF7 in the presence or absence of MG132, followed by infection with vA187-1 or C<sub>112</sub>R mutant CSFV. Comparable levels of IRF7 were detected in mock-, CSFV-, and C<sub>112</sub>R mutant-infected cells at each time point in the absence of MG132 (Fig. 4B, bottom panel). The decrease of IRF7 in all samples at 24 h after infection is consistent with the known high turnover of IRF7. Note that in the presence of MG132, the overall IRF7 expression levels were low (Fig. 4B, top panel), probably due to the toxic effect of MG132. From previous data we know that the level of IRF3 is clearly reduced at 24 h after infection with vA187-1 and can be rescued by inhibition of the proteasomal activity (6). Here we show that in contrast to the case for IRF3, the amount of IRF7 was not influenced by infection with either

vA187-1 or the C<sub>112</sub>R mutant virus. In conclusion, in SK-6 cells there is no evidence of accelerated proteasomal degradation of IRF7 resulting from the interaction of N<sup>PRO</sup> with IRF7.

**The interaction of N<sup>PRO</sup> with IRF7 results in reduced CSFV-induced IFN-α responses in pDC.** pDC are considered to be the main source of the high serum levels of IFN-α found during the first 2 to 5 days after CSFV infection *in vivo* (29, 51), and they are known to respond to viruses in an IRF3-independent, IRF7-dependent pathway (24). Therefore, we analyzed the induction of IFN-α in enriched porcine pDC at different times after infection with wild-type CSFV or with CSFV carrying the D<sub>136</sub>N or the C<sub>112</sub>R mutation in N<sup>PRO</sup>, abolishing the interaction of N<sup>PRO</sup> with IRF7. No IFN-α was observed in mock-treated cells, whereas infection with wild-type CSFV resulted in the production of low levels of IFN-α found at 6 h, 24 h, and 48 h postinfection (p.i.) (Fig. 5A). Related to their inability to interact with IRF7, the D<sub>136</sub>N or C<sub>112</sub>R mutant CSFV led to a 5-fold-higher production of IFN-α. Independently of the virus dose, the relative difference in the induction of IFN-α between the wild-type and the D<sub>136</sub>N mutant viruses remained visible (Fig. 5B). The differences between wild-type and N<sup>PRO</sup> mutant CSFV in the induction of IFN-α were also observed in the context of the highly virulent Eystrup strain (Fig. 5C). Interestingly, the latter virus consistently induced higher levels of IFN-α than the moderately virulent vA187-1 strain. At the IFN-α and IFN-β mRNA levels, the D<sub>136</sub>N and C<sub>112</sub>R mutants also induced higher responses than the wild-

FIG. 3. Truncations at the amino terminus or the carboxy terminus of IRF3 and IRF7 affect the interaction with N<sup>PRO</sup>. (A) Schematic representation of porcine IRF3 and IRF7 based on the domain prediction tool SMART; the DNA-binding domain (DNA-BD) and the regulatory domain (RD) are indicated. (B) Schematic representation of the N-terminal and C-terminal deletion mutants of IRF3 and IRF7; all the truncated fragments were expressed fused to the C terminus of the transactivator VP16 of the pFN10A(ACT) plasmid. (C and D) The expression of IRF3 (C) and IRF7 (D) and of mutants thereof was analyzed by Western blotting and detection with rabbit antisera against porcine IRF3 and IRF7, respectively. The α-tubulin content was determined as a loading control using the anti-α-tubulin MAb. (E and F) The interaction of N<sup>PRO</sup> with the truncated forms of IRF3 (E) and IRF7 (F) was analyzed using the mammalian two-hybrid assay. HEK293T cells were transfected with plasmids for the expression of the GAL4-N<sup>PRO</sup> chimeric protein and of the VP16-IRF3 (E) or VP16-IRF7 (F) proteins and the indicated deletion mutants. The fold induction of firefly luciferase activity normalized to *Renilla* luciferase activity was calculated relative to the negative-control pACT and pBIND. The error bars represent the standard deviation.

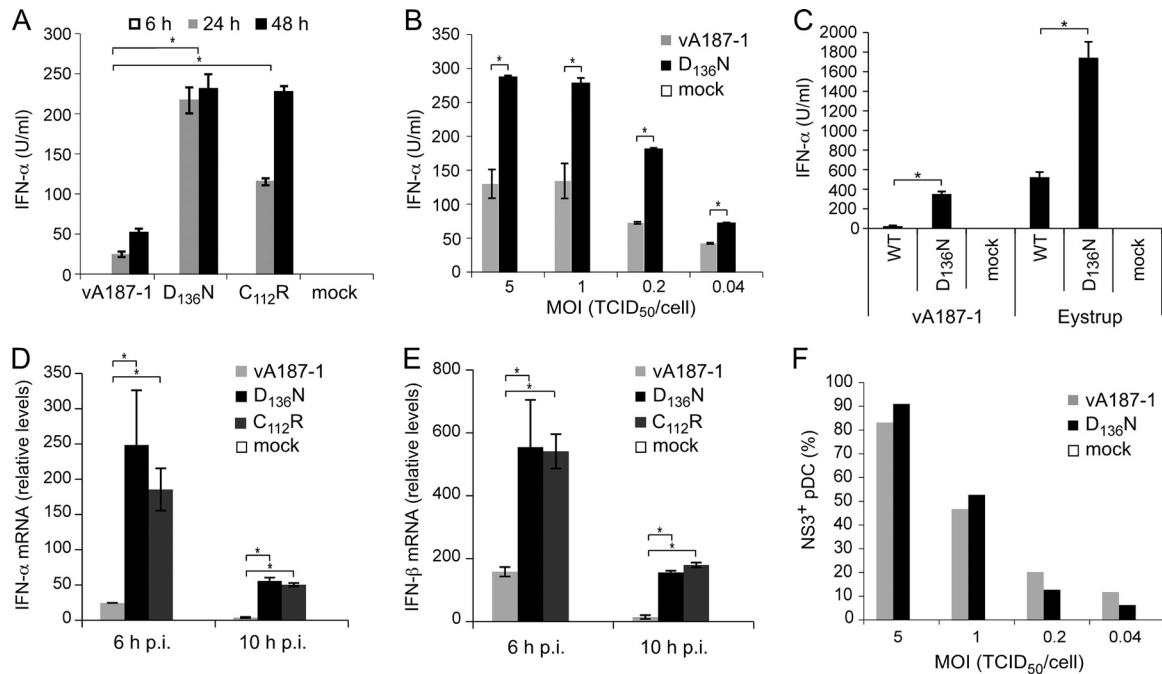


FIG. 5.  $N^{\text{pro}}$  limits the IFN- $\alpha$  responses in pDC. (A) Enriched pDC were mock treated or infected at a MOI of 2 TCID<sub>50</sub>/cell with CSFV strain vA187-1 or with CSFV vA187-1 carrying the C<sub>112</sub>R or the D<sub>136</sub>N mutation in  $N^{\text{pro}}$ . The supernatants were collected at 6, 24, and 48 h p.i., and IFN- $\alpha$  was measured by ELISA. The bars show the means of triplicates from a representative experiment, with error bars showing the standard deviation. (B) Enriched pDC were mock treated or infected with CSFV vA187-1 or with the D<sub>136</sub>N mutant at an MOI of 5, 2, 1, or 0.04 TCID<sub>50</sub>/cell. Supernatants were collected at 20 h p.i., and IFN- $\alpha$  was quantified by ELISA. (C) Enriched pDC were mock treated or infected at an MOI of 1 TCID<sub>50</sub>/cell with the wild-type (WT) CSFV strains vA187-1 or Eystруп as indicated, and with the respective D<sub>136</sub>N mutant viruses. The supernatants were collected at 20 h p.i., and IFN- $\alpha$  was measured by ELISA. (D and E) The contents of IFN- $\alpha$  (D) and IFN- $\beta$  (E) mRNAs of purified pDC at different times after mock treatment or infection with CSFV strain vA187-1 or the D<sub>136</sub>N and C<sub>112</sub>R mutants were measured by real time RT-PCR. The amount of mRNA is shown relative to the levels of the 18S mRNA. (F) Enriched pDC were mock treated or infected with CSFV vA187-1 or the D<sub>136</sub>N mutant at an MOI of 5, 2, 1, or 0.04 TCID<sub>50</sub>/cell. At 20 h p.i., triple staining for surface CD172a, CD4, and intracellular NS3 was performed. The percentage of NS3-positive cells was calculated on CD172a<sup>low</sup> CD4<sup>+</sup> pDC. The results of one representative experiment out of three are shown. Statistically significant differences ( $P < 0.05$ , calculated by Student's  $t$  test) are shown with an asterisk.

type CSFV at 6 and 10 h p.i. (Fig. 5D and E). The ability of the  $N^{\text{pro}}$  mutants to induce higher IFN- $\alpha/\beta$  responses than the wild-type CSFV was not due to different levels of infection by the viruses, since the percentages of NS3<sup>+</sup> pDC were comparable at various virus doses (Fig. 5F). Taken together, the results show that CSFV has the ability to significantly limit IFN- $\alpha/\beta$  induction in pDC and that this function is mediated by the viral protein  $N^{\text{pro}}$ , probably through its ability to interfere with IRF3 and/or IRF7 signaling.

**$N^{\text{pro}}$  negatively regulates IRF7 levels in pDC.** In order to determine the mechanisms by which  $N^{\text{pro}}$  limits the production of IFN- $\alpha$  in pDC, we examined the fate of IRF7 following infection of purified pDC with wild-type and with D<sub>136</sub>N and C<sub>112</sub>R mutant CSFV. With no IRF7 detectable in mock-infected cells, the D<sub>136</sub>N mutant induced a strong upregulation of IRF7 that was visible with the first IFN- $\alpha$  found at 6 h p.i. In wild-type-infected pDC, IRF7 was detectable as a weak band in the Western blot as early as 6 h p.i. Interestingly, despite the high levels of IFN- $\alpha$  (several thousand units) also found in the wild-type CSFV-infected purified pDC cultures at 10 h and 24 h p.i., the IRF7 levels remained at a constant low level and never reached the high levels found in pDC infected with the D<sub>136</sub>N mutant virus (Fig. 6A). These observations were confirmed by flow cytometry. While infection with the parent

CSFV resulted in IRF7 expression similar to that with mock infection (Fig. 6B, right panel), the D<sub>136</sub>N and C<sub>112</sub>R mutant CSFV induced higher levels of IRF7. In addition, we observed a clear reduction of IRF3 expression in wild-type CSFV-infected pDC compared with mock treatment or infection with D<sub>136</sub>N and C<sub>112</sub>R mutant CSFV (Fig. 6B, left panel), confirming previous data showing the degradation of IRF3 in other cell types (6). In order to determine whether the differences in the IRF7 protein expression levels seen in Fig. 6A and B resulted from different transcriptional activities, we quantified IRF3 and IRF7 mRNAs by real-time RT-PCR in wild-type CSFV-infected pDC versus pDC infected with D<sub>136</sub>N mutant CSFV. IRF7 was strongly induced by both wild-type and mutant CSFV. Although at 10 h p.i., the D<sub>136</sub>N mutant induced higher levels of IRF7, with both viruses similar maximum levels of 170- to 190-fold over that with the mock controls were found (Fig. 6C). Compared to that of IRF7, the induction of IRF3 was lower, and no difference was found between the wild type and the  $N^{\text{pro}}$  mutant at most time points analyzed (Fig. 6D). The higher levels of IRF3 induced by vA187-1 found at 16 h p.i. were not reproducible. From this we conclude that the lower IRF7 protein levels found in wild-type CSFV infection did not result from lower transcription. Taken together, these findings indicate that  $N^{\text{pro}}$  negatively regulates IRF7 at the

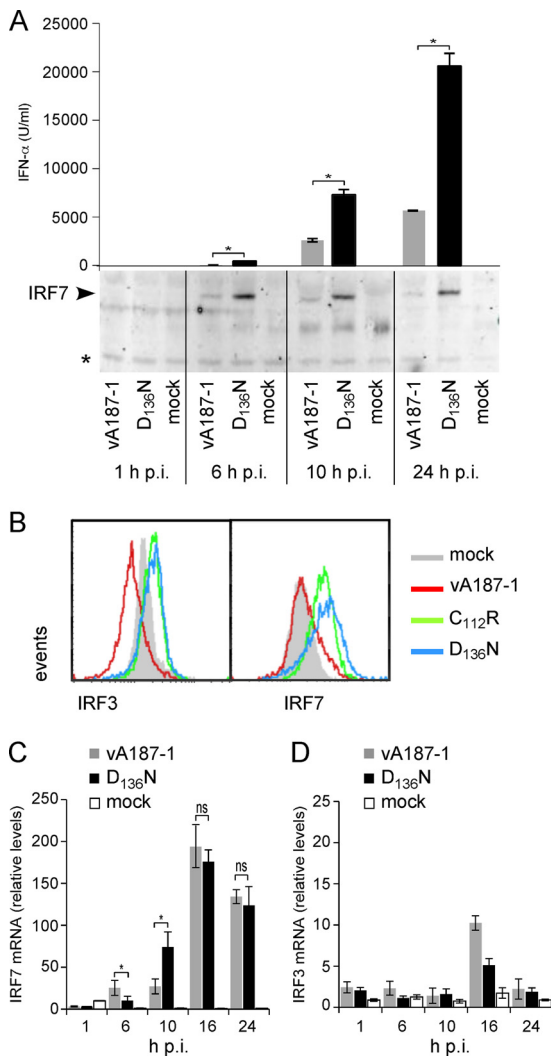


FIG. 6. N<sup>pro</sup> negatively regulates the IRF7 protein but not the IRF7 mRNA levels in pDC. (A) Purified pDC were mock treated or infected with CSFV vA187-1 or the D<sub>136</sub>N mutant at an MOI of 2 TCID<sub>50</sub>/cell. The supernatants were collected at 1, 6, 10, and 24 h p.i., and IFN-α was measured by ELISA. The bars show the means of triplicates from one representative experiment out of three, with error bars displaying the standard deviation. In parallel, the expression of IRF7 from the same wells was analyzed by Western blotting and detection with rabbit antiserum against the porcine IRF7 (the asterisk indicates an unspecific band shown as loading control). (B) Enriched pDC were mock treated or infected with CSFV vA187-1 or with the C<sub>112</sub>R or the D<sub>136</sub>N mutant at an MOI of 1 TCID<sub>50</sub>/cell. At 20 h p.i., triple staining was performed for surface CD172a and CD4 and for intracellular IRF3 (left panel) or IRF7 (right panel). The CD172<sup>low</sup> CD4<sup>+</sup> pDC subset was analyzed for IRF3 (left panel) and IRF7 (right panel) expression. The results of one representative experiment out of two are shown. (C and D) Purified pDC were mock treated or infected with CSFV strain vA187-1 or with the D<sub>136</sub>N mutant at an MOI of 1 TCID<sub>50</sub>/cell. The levels of IRF7 (C) and IRF3 (D) mRNAs relative to the 18S mRNA were measured by real-time RT-PCR at 1, 6, 10, 16, and 24 h p.i. The bars show the means for triplicate cultures from one representative experiment out of three. In panels A and C, statistically significant differences ( $P < 0.05$ , calculated by Student's *t* test) are shown with an asterisk. ns, not significant.

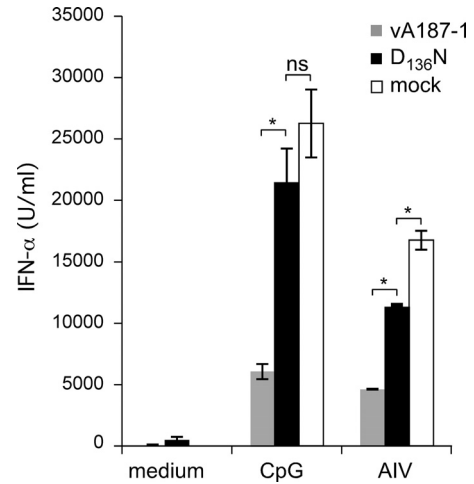


FIG. 7. Infection with CSFV but not with virus carrying the D<sub>136</sub>N mutation in N<sup>pro</sup> inhibits the IFN-α response in pDC. Enriched pDC were mock treated or infected with CSFV vA187-1 or vA187-D<sub>136</sub>N at an MOI of 2 TCID<sub>50</sub>/cell. At 18 h p.i., the cells were stimulated by adding CpG 2216 (10 μg/ml) to the cell culture medium or by infection with H5N1 AIV at an MOI of 10 TCID<sub>50</sub>/cell. The supernatants were collected after 24 h and tested for IFN-α by ELISA. Statistically significant differences ( $P < 0.05$ , calculated by Student's *t* test) are shown with an asterisk. ns, not significant.

protein level in pDC, probably through interference with IRF7 turnover.

**Infection with CSFV inhibits the IFN-α response in pDC.** In order to investigate whether CSFV can also inhibit the IFN-α response of pDC to other TLR ligands or viruses, we infected enriched pDC with wild-type and D<sub>136</sub>N mutant CSFV for 20 h and subsequently treated the cells with CpG as a TLR9 agonist or with H5N1 AIV as a TLR7 agonist (Fig. 7). Interestingly, infection with parental CSFV impaired the ability of pDC to secrete high levels of IFN-α in response to the other stimuli. In pDC infected with D<sub>136</sub>N mutant CSFV, this inhibition was not observed with CpG stimulation and was significantly less potent for AIV activation. These data demonstrate that CSFV is able to negatively regulate the IFN-α response in pDC, presumably through its ability to reduce the levels of IRF7.

DISCUSSION

N<sup>pro</sup> of pestiviruses antagonizes the induction of the early innate immune response in non-pDC such as epithelial cells, macrophages, and monocyte-derived DC. This function is related to a Zn-binding motif in the C-terminal half of N<sup>pro</sup> that is essential for N<sup>pro</sup> to interact with IRF3, resulting in the proteasomal degradation of IRF3 (53). Considering that in mouse pDC type I IFN induction was found to be essentially IRF7 dependent (24), it was not surprising to observe that pDC represent the only cell type able to respond to CSFV infection by production of IFN-α (4, 6, 8, 35). However, here we demonstrate a novel function of N<sup>pro</sup> in innate immunity, namely, its interaction with IRF7, which reduces IRF7-dependent IFN-α induction in SK-6 cells and pDC.

In contrast to other cells, human pDC express IRF7 constitutively, although this basal expression is rapidly upregulated after stimulation (28, 34, 54) and is maintained *in vitro* only in

the presence of a stimulant (12). Related to this, studies with human pDC describe that nuclear translocation of IRF7 occurs earlier than IRF7 induction, implying that the first wave of IFN- $\alpha$  is induced by the constitutively expressed IRF7 in pDC (12, 54). This would explain our finding that CSFV induces considerable amounts of IFN- $\alpha$  despite the interference of N<sup>PtO</sup> with IRF3 and IRF7 functions. However, the IFN- $\alpha$  levels found with the Zn-binding-deficient N<sup>PtO</sup> are never reached during infection with the parent CSFV due to a limited IRF7 expression observed with CSFV infection. Our data with pDC suggest that IRF7 is regulated at the protein level, since no or only minor differences were found in the IRF7 mRNA quantities. In the porcine cell lines SK-6 and PK-15, endogenous IRF7 protein was not detectable. Our results obtained with SK-6 cells expressing plasmid-driven IRF7 did not show any evidence of accelerated proteasomal degradation of IRF7, supporting earlier studies in which a downregulation of IRF7 expression in PK-15 cells was not detected (6). Nevertheless, it is clear from this study that under "natural" conditions in pDC, functional N<sup>PtO</sup> limits the level of IRF7 protein, which in turn limits IFN- $\alpha$  induction. However, it is not clear whether N<sup>PtO</sup> accelerates proteasomal degradation of IRF7 in pDC or whether alternative mechanisms are involved. Experiments with proteasome inhibitors such as MG132 and epoxomycin did not answer this question due to the toxicity of these drugs in pDC. It is possible that N<sup>PtO</sup> utilizes a different mechanism to interfere with IRF7 than to interfere with IRF3. An alternative could be that N<sup>PtO</sup> influences the localization of IRF7 and retains the transcription factor in the cytoplasm, as has been reported, for example, in the context of hepatitis C virus (40). A reduced translocation of IRF7 following CSFV infection not only may result in a reduction of IFN- $\alpha$  induction but also may modulate the overall natural proteasome-mediated IRF7 turnover in the infected pDC.

Several examples in the literature demonstrate that viral proteins interfere with the induction of type I IFN by antagonizing the function of multiple IRFs (5, 7). One explanation for this might be that the members of the IRF family contain related features, including an N-terminal DNA-binding domain (55). As shown here, porcine IRF3 and IRF7 share at least structural elements, namely, the N-terminal DNA-binding domain and a regulatory domain in the C-terminal half of the protein. This led us to hypothesize that N<sup>PtO</sup> may interact with a common domain in certain IRF family members. However, mutational analyses indicate that N<sup>PtO</sup> does not interact with IRF3 and IRF7 upon recognition of a single domain but that nearly the complete IRF protein is necessary for full interaction. Importantly, N<sup>PtO</sup> relies on an intact Zn-binding domain for the interaction with IRF7, as with IRF3. These data provide a further indication that N<sup>PtO</sup> uses partially overlapping but distinct mechanisms to interact with IRF3 and IRF7.

Our results add a new piece of information to understand the mechanisms involved in the pathogenesis of CSF. At the initial sites of replication, involving macrophages, conventional DCs, and endothelial and epithelial cells, CSFV N<sup>PtO</sup> would inhibit viral RNA-induced IFN- $\alpha/\beta$  production, allowing the virus to rapidly replicate and resulting in viremia and spread to secondary sites of replication. By targeting IRF3 for degradation, N<sup>PtO</sup> removes an upstream transcription factor needed for

inducing the IRF7-dependent IFN- $\alpha/\beta$  feedback loop, which is essential in non-pDC (25). As the speed and level of replication are critical for the outcome of the disease, this inhibition of the innate immune response would allow CSFV to establish a productive infection. Once the virus has spread to secondary sites of replication representing lymphoid tissue, it would infect pDC that can produce IFN- $\alpha$  independently of IRF3 (24). This activation of pDC would result in the production of pro-inflammatory cytokines and IFN- $\alpha$  related to the typical immunopathological syndrome of CSF (3, 43, 51). In this context it is important to note that the IFN- $\alpha$  responses during CSF are correlated with the severity of the disease (29, 43, 51). We speculate that in this phase of acute disease the interaction of N<sup>PtO</sup> with IRF7 could be beneficial to limit IFN- $\alpha$  and cytokine responses. This would explain earlier results showing disease exacerbation with increased serum IFN- $\alpha$  levels in pigs infected with the highly virulent vEy-37 strain in which the Zn-binding function of N<sup>PtO</sup> was knocked out (43). It could thus be of evolutionary benefit for the virus to establish more chronic persisting infections rather than peracute disease with rapid death of the animals, as a consequence of "cytokine storm" and shock typical of severe hemorrhagic fevers. However, it is important to note that the influence of N<sup>PtO</sup> on the outcome of the infection is not absolute but acts in concert with other virulence factors, as the impact of N<sup>PtO</sup> in the pathogenesis differs between moderate and highly virulent strains (43).

Taken together, our results present a novel function of N<sup>PtO</sup> in subverting the innate immune system. Considering that IRF3 is the initial trigger of IFN- $\beta$  expression and IRF7, the "master regulator" of type I IFN (25), the dual actions of N<sup>PtO</sup> would help the virus to interfere with autocrine and paracrine pathways of type I IFN induction in a cell type-dependent manner. In the future it will be of interest to study whether N<sup>PtO</sup> is also capable of interacting with other members of the IRF family and to define the molecular mechanisms in more detail. Understanding of the diverse molecular interactions of CSFV with targets of the innate immune system will help us to gain a closer insight into pathogenesis and to understand virus-host coevolution of CSF and other hemorrhagic fevers.

#### ACKNOWLEDGMENTS

This work was supported by Swiss National Science Foundation grants 31003A-116608 and 310030-116800.

We thank Irene Greiser-Wilke (Hannover Veterinary School, Hannover, Germany) for MAb C16, Martin D. Fray (Institute of Animal Health, Compton, Newbury, Berkshire, United Kingdom) for the Mx/CAT reporter gene assay, Armin Saalmüller (Institute of Immunology, Department of Pathobiology, University of Veterinary Medicine Vienna, Vienna, Austria) for the hybridomas for MAbs 74-22-15A and 74-12-4, Karin Haverson (University of Bristol, United Kingdom) for the hybridoma for MAb PTT3, Bernard Charley (INRA, Jouy-en-Josas, France) for the anti-pig IFN- $\alpha$  MAbs K9 and F17, and Jim Robertson (National Institute for Biological Standards and Control, Hertfordshire, United Kingdom) for the AIV H5N1 NIBRG14. We also thank Jon Duri Tratschin for critical reading of the manuscript and Christian Griot, Director of IVI, for continuous support.

#### REFERENCES

- Au, W. C., W. S. Yeow, and P. M. Pitha. 2001. Analysis of functional domains of interferon regulatory factor 7 and its association with IRF-3. *Virology* **280**:273-282.
- Baigent, S. J., S. Goodbourn, and J. W. McCauley. 2004. Differential activation of interferon regulatory factors-3 and -7 by non-cytopathogenic and cytopathogenic bovine viral diarrhoea virus. *Vet. Immunol. Immunopathol.* **100**:135-144.

3. **Balmelli, C., N. Ruggli, K. McCullough, and A. Summerfield.** 2005. Fibrocytes are potent stimulators of anti-virus cytotoxic T cells. *J. Leukoc. Biol.* **77**:923–933.
4. **Balmelli, C., et al.** 2005. FcγRII-dependent sensitisation of natural interferon-producing cells for viral infection and interferon-α responses. *Eur. J. Immunol.* **35**:2406–2415.
5. **Barro, M., and J. T. Patton.** 2007. Rotavirus NSP1 inhibits expression of type I interferon by antagonizing the function of interferon regulatory factors IRF3, IRF5, and IRF7. *J. Virol.* **81**:4473–4481.
6. **Bauhofer, O., et al.** 2007. N<sup>PRO</sup> of classical swine fever virus interacts with interferon regulatory factor 3 and induces its proteasomal degradation. *J. Virol.* **81**:3087–3096.
7. **Bentz, G. L., R. Liu, A. M. Hahn, J. Shackelford, and J. S. Pagano.** 2010. Epstein-Barr virus BRLF1 inhibits transcription of IRF3 and IRF7 and suppresses induction of interferon-β. *Virology* **402**:121–128.
8. **Carrasco, C. P., et al.** 2001. Porcine dendritic cells generated in vitro: morphological, phenotypic and functional properties. *Immunology* **104**:175–184.
9. **Chen, Z., et al.** 2007. Ubiquitination and proteasomal degradation of interferon regulatory factor-3 induced by N<sup>PRO</sup> from a cytopathic bovine viral diarrhoea virus. *Virology* **366**:277–292.
10. **Cheng, T. F., et al.** 2006. Differential activation of IFN regulatory factor (IRF)-3 and IRF-5 transcription factors during viral infection. *J. Immunol.* **176**:7462–7470.
11. **Childs, K., et al.** 2007. mda-5, but not RIG-I, is a common target for paramyxovirus V proteins. *Virology* **359**:190–200.
12. **Dai, J. H., N. J. Megjugorac, S. B. Amrute, and P. FitzgeraldBocarsly.** 2004. Regulation of IFN regulatory factor-7 and IFN-α production by enveloped virus and lipopolysaccharide in human plasmacytoid dendritic cells. *J. Immunol.* **173**:1535–1548.
13. **Fitzgerald, K. A., et al.** 2003. IKKε and TBK1 are essential components of the IRF3 signaling pathway. *Nat. Immunol.* **4**:491–496.
14. **Fray, M. D., G. E. Mann, and B. Charleston.** 2001. Validation of an Mx/CAT reporter gene assay for the quantification of bovine type-I interferon. *J. Immunol. Methods* **249**:235–244.
15. **Goodbourn, S., L. Didcock, and R. E. Randall.** 2000. Interferons: cell signalling, immune modulation, antiviral response and virus countermeasures. *J. Gen. Virol.* **81**:2341–2364.
16. **Greiser-Wilke, I., K. E. Dittmar, B. Liess, and V. Moennig.** 1992. Heterogeneous expression of the non-structural protein p80/p125 in cells infected with different pestiviruses. *J. Gen. Virol.* **73**:47–52.
17. **Guzylack-Piriou, L., F. Bergamin, M. Gerber, K. C. McCullough, and A. Summerfield.** 2006. Plasmacytoid dendritic cell activation by foot-and-mouth disease virus requires immune complexes. *Eur. J. Immunol.* **36**:1674–1683.
18. **Guzylack-Piriou, L., C. Balmelli, K. C. McCullough, and A. Summerfield.** 2004. Type-A CpG oligonucleotides activate exclusively porcine natural interferon-producing cells to secrete interferon-α, tumour necrosis factor-α and interleukin-12. *Immunology* **112**:28–37.
19. **Haller, O., G. Kochs, and F. Weber.** 2006. The interferon response circuit: induction and suppression by pathogenic viruses. *Virology* **344**:119–130.
20. **Hata, N., et al.** 2001. Constitutive IFN-α/β signal for efficient IFN-α/β gene induction by virus. *Biochem. Biophys. Res. Commun.* **285**: 518–525.
21. **Hengel, H., U. H. Koszinowski, and K. K. Conzelmann.** 2005. Viruses know it all: new insights into IFN networks. *Trends Immunol.* **26**:396–401.
22. **Hertzog, P. J., L. A. O'Neill, and J. A. Hamilton.** 2003. The interferon in TLR signaling: more than just antiviral. *Trends Immunol.* **24**:534–539.
23. **Hilton, L., et al.** 2006. The N<sup>PRO</sup> product of bovine viral diarrhoea virus inhibits DNA binding by interferon regulatory factor 3 and targets it for proteasomal degradation. *J. Virol.* **80**:11723–11732.
24. **Honda, K., et al.** 2005. IRF-7 is the master regulator of type-I interferon-dependent immune responses. *Nature* **434**:772–777.
25. **Honda, K., H. Yanai, A. Takaoka, and T. Taniguchi.** 2005. Regulation of the type I IFN induction: a current view. *Int. Immunol.* **17**:1367–1378.
26. **Huang, B., Z. T. Qi, Z. Xu, and P. Nie.** 2010. Global characterization of interferon regulatory factor (IRF) genes in vertebrates: glimpse of the diversification in evolution. *BMC Immunol.* **11**:22.
27. **Island, M. L., et al.** 2002. Repression by homeoprotein pitx1 of virus-induced interferon promoters is mediated by physical interaction and trans repression of IRF3 and IRF7. *Mol. Cell. Biol.* **22**:7120–7133.
28. **Izaguirre, A., et al.** 2003. Comparative analysis of IRF and IFN-α expression in human plasmacytoid and monocyte-derived dendritic cells. *J. Leukoc. Biol.* **74**:1125–1138.
29. **Jamin, A., S. Gorin, R. Cariolet, M. F. Le Potier, and G. Kuntz-Simon.** 2008. Classical swine fever virus induces activation of plasmacytoid and conventional dendritic cells in tonsil, blood, and spleen of infected pigs. *Vet. Res.* **39**:7.
30. **Kasza, L., J. A. Shaddock, and G. J. Christofinis.** 1972. Establishment, viral susceptibility and biological characteristics of a swine kidney cell line SK-6. *Res. Vet. Sci.* **13**:46–51.
31. **Kato, H., et al.** 2005. Cell type-specific involvement of RIG-I in antiviral response. *Immunity* **23**:19–28.
32. **Kawai, T., and S. Akira.** 2006. Innate immune recognition of viral infection. *Nat. Immunol.* **7**:131–137.
33. **Kawai, T., et al.** 2004. Interferon-α induction through Toll-like receptors involves a direct interaction of IRF7 with MyD88 and TRAF6. *Nat. Immunol.* **5**:1061–1068.
34. **Kerkmann, M., et al.** 2003. Activation with CpG-A and CpG-B oligonucleotides reveals two distinct regulatory pathways of type I IFN synthesis in human plasmacytoid dendritic cells. *J. Immunol.* **170**:4465–4474.
35. **Knoetig, S. M., A. Summerfield, M. Spagnuolo-Weaver, and K. C. McCullough.** 1999. Immunopathogenesis of classical swine fever: role of monocyte cells. *Immunology* **97**:359–366.
36. **Lin, R., P. Genin, Y. Mamane, and J. Hiscott.** 2000. Selective DNA binding and association with the CREB binding protein coactivator contribute to differential activation of α/β interferon genes by interferon regulatory factors 3 and 7. *Mol. Cell. Biol.* **20**:6342–6353.
37. **Lubyova, B., M. J. Kellum, A. J. Frisancho, and P. M. Pitha.** 2004. Kaposi's sarcoma-associated herpesvirus-encoded vIRF-3 stimulates the transcriptional activity of cellular IRF-3 and IRF-7. *J. Biol. Chem.* **279**:7643–7654.
38. **Malmgaard, L.** 2004. Induction and regulation of IFNs during viral infections. *J. Interferon Cytokine Res.* **24**:439–454.
39. **Quevillon, E., et al.** 2005. InterProScan: protein domains identifier. *Nucleic Acids Res.* **33**:W116–W120.
40. **Raychoudhuri, A., et al.** 2010. Hepatitis C virus infection impairs IRF-7 translocation and alpha interferon synthesis in immortalized human hepatocytes. *J. Virol.* **84**:10991–10998.
41. **Rottenberg, S., J. Schmuckli-Maurer, S. Grimm, V. T. Heussler, and D. A. Dobbelaer.** 2002. Characterization of the bovine IkappaB kinases (IKK)α and IKKβ, the regulatory subunit NEMO and their substrate IkappaBα. *Gene* **299**:293–300.
42. **Ruggli, N., et al.** 2005. N<sup>PRO</sup> of classical swine fever virus is an antagonist of double-stranded RNA-mediated apoptosis and IFN-α/β induction. *Virology* **340**:265–276.
43. **Ruggli, N., et al.** 2009. Classical swine fever virus can remain virulent after specific elimination of the interferon regulatory factor 3-degrading function of Npro. *J. Virol.* **83**:817–829.
44. **Ruggli, N., et al.** 2003. Classical swine fever virus interferes with cellular antiviral defense: evidence for a novel function of N<sup>PRO</sup>. *J. Virol.* **77**:7645–7654.
45. **Sato, M., et al.** 2000. Distinct and essential roles of transcription factors IRF-3 and IRF-7 in response to viruses for IFN-α/β gene induction. *Immunity* **13**:539–548.
46. **Schultz, J., F. Milpetz, P. Bork, and C. P. Ponting.** 1998. SMART, a simple modular architecture research tool: identification of signaling domains. *Proc. Natl. Acad. Sci. U. S. A.* **95**:5857–5864.
47. **Schwartz-Cornil, L., M. Eparaud, and M. Bonneau.** 2006. Cervical duct cannulation in sheep for collection of afferent lymph dendritic cells from head tissues. *Nat. Protoc.* **1**:874–879.
48. **Seago, J., et al.** 2007. The N<sup>PRO</sup> product of classical swine fever virus and bovine viral diarrhoea virus uses a conserved mechanism to target interferon regulatory factor-3. *J. Gen. Virol.* **88**:3002–3006.
49. **Servant, M. J., B. Tenoever, and R. Lin.** 2002. Overlapping and distinct mechanisms regulating IRF-3 and IRF-7 function. *J. Interferon Cytokine Res.* **22**:49–58.
50. **Sharma, S., et al.** 2003. Triggering the interferon antiviral response through an IKK-related pathway. *Science* **300**:1148–1151.
51. **Summerfield, A., M. Alves, N. Ruggli, M. G. de Bruin, and K. C. McCullough.** 2006. High IFN-α responses associated with depletion of lymphocytes and natural IFN-producing cells during classical swine fever. *J. Interferon Cytokine Res.* **26**:248–255.
52. **Summerfield, A., et al.** 2003. Porcine peripheral blood dendritic cells and natural interferon-producing cells. *Immunology* **110**:440–449.
53. **Szymanski, M. R., et al.** 2009. Zinc binding in pestivirus N<sup>PRO</sup> is required for interferon regulatory factor 3 interaction and degradation. *J. Mol. Biol.* **391**:438–449.
54. **Takauji, R., et al.** 2002. CpG-DNA-induced IFN-α production involves p38 MAPK-dependent STAT1 phosphorylation in human plasmacytoid dendritic cell precursors. *J. Leukoc. Biol.* **72**:1011–1019.
55. **Taniguchi, T., K. Ogasawara, A. Takaoka, and N. Tanaka.** 2001. IRF family of transcription factors as regulators of host defense. *Annu. Rev. Immunol.* **19**:623–655.
56. **Uematsu, S., et al.** 2005. Interleukin-1 receptor-associated kinase-1 plays an essential role for Toll-like receptor (TLR)7- and TLR9-mediated interferon-α induction. *J. Exp. Med.* **201**:915–923.
57. **Weber, F., G. Kochs, and O. Haller.** 2004. Inverse interference: how viruses fight the interferon system. *Viral Immunol.* **17**:498–515.
58. **Yoneyama, M., et al.** 1998. Direct triggering of the type I interferon system by virus infection: activation of a transcription factor complex containing IRF-3 and CBP/p300. *EMBO J.* **17**:1087–1095.